

Determination of the age of the earth from Kamland measurement of geo-neutrinos

Subhendra Mohanty

Physical Research Laboratory, Ahmedabad 380009, India.

(Dated: October 31, 2018)

The low energy component of the anti-neutrino spectrum observed in the recent Kamland experiment has significant contribution from the radioactive decay of ^{238}U and ^{232}Th in the earth. By taking the ratio of the anti-neutrino events observed in two different energy ranges we can determine the present value of the Thorium by Uranium abundance ratio, independent of the U,Th distribution in the earth. Comparing the present abundance ratio with the r-process predicted initial value we determine the age of the earth as a function of Δm^2 and $\text{Sin}^2 2\theta$. We find that the age of the earth determined from KamLAND data matches the age of solar system (4.5Gyrs determined from meteorites) for the LMA-I solution. For the LMA-II solution the age of the earth does not match the solar system age even at 90%C.L.

PACS numbers:

The recent results from KamLAND [1] are significant for establishing the LMA solution of the solar neutrino problem. In addition they present the first statistically significant measurement the anti-neutrinos from radioactive decay of ^{238}U and ^{232}Th present in the crust and mantle of the earth. The possibility of detecting geo neutrinos from radioactivity in the the earth was first raised by Eder [2] and was revived by Krauss et al [3] and Kobayashi and Fukao [4]. Quantitative spectra of the anti-neutrino events which could be observed at Kamioka and Gran Sasso from radioactivity of Th and U in the earth has been given by Rothschild et al [5] and Raghavan et al [6]. The emphasis of these papers and the recent work of Fiorentini et al [7] is to use the observations of $\bar{\nu}_e$ events at KamLAND and Borexino experiments to determine the distribution of U, Th in the crust and mantle of the earth, and determine what fraction of the 40TW heat generated by earth from radioactivity. KamLAND [1] reports observing 9 $\bar{\nu}_e$ events below 2.6MeV (visible positron energy) which are ascribed to U, Th radioactivity in the earth. Subsequently a analysis of the geo neutrinos from KamLAND observations has been done by Fiorentini et al [8] with the aim of determining the geological distribution of U and Th in the earth. Fiorentini et al. assume that $[\text{Th}/\text{U}] = 3.8$ the solar system value and try to determine the U and Th content of the core and mantle.

In this paper we have a different aim which is to extract the average thorium by uranium abundance ratio, $[\text{Th}/\text{U}]$ from the KamLAND data, as this parameter is an ideal chronometer for measurement of cosmological time-scales. Th and U present in the earth are produced in supernova by r-process nucleosynthesis [9]. The theoretical prediction initial abundance ratio is robust against perturbations of the astrophysical parameters at the site of the r-process to within $\pm 5\%$ [10]. By determining the present abundance ratio of $[\text{Th}/\text{U}]$ in the earth from KamLAND, we can measure the age of the earth-i.e the time elapsed between the supernova explosion where the Th and U in the earth were produced, and the present.

KamLAND observes geo anti-neutrinos in the (positron signal) energy range $0.9\text{MeV} < E < 2.5\text{MeV}$. Thorium decay neutrinos have a maximum E value of 1.5MeV whereas Uranium neutrinos contribute in the entire observed energy range of the geo signal. The geo neutrinos undergo an energy independent suppression as their average distance from the detector $\sim 10^3\text{km}$ is much larger than the oscillation length $\sim 10^2\text{km}$. We take the ratio of the geo events, in the the $(0.9 - 1.5)\text{MeV}$ bins and the geo events, in the $(1.5 - 2.5)\text{MeV}$ energy bins to determine the $[\text{Th}]/[\text{U}]$. This enables us to determine the age of the earth independent of the geological distribution of Th and U in the earth.

Using the KamLAND data we can determine the age of the earth as a function of Δm^2 and $\text{Sin}^2 2\theta$, as these parameters determine the reactor background that has to be subtracted from the KamLAND observed events to arrive at the geo-neutrino signal. In Fig.1 we show the age of the earth as a function of the mixing angle for the LMA-I ($\Delta m^2 = 7 \times 10^{-5}\text{eV}^2$) and LMA-II ($\Delta m^2 = 15 \times 10^{-5}\text{eV}^2$) solutions [11]. We estimate the total uncertainty in the age (for a given $\Delta m^2, \text{Sin}^2 2\theta$) to be $\pm 36.5\%$. The central shaded regions are the best fit points ($\chi^2 \sim 0$) and the two outer lines enclose the allowed region of parameter space with C.L. of 68.3% and 90% respectively. We see from Fig.1 that for the LMA-II solution $t_{\text{age}} > 5.0\text{Gyrs}$ (at 90%C.L) and $t_{\text{age}} > 9.0\text{Gyrs}$ (at 68.3%C.L) . It is known from the radiochemical dating of meteorites that the age of the oldest meteorites (the chondrites) is 4.5Gyrs [12]. If the age of the earth is close to the age of the chondrites then the LMA-II solution is ruled out. We see from Fig1 that for the LMA-I solution, the age of the earth agrees with the age of the meteorites for the mixing angle in the range $0.88 < \text{Sin}^2 2\theta < 0.93$.

The KamLAND detector consists of about 1kiloton of liquid scintillator surrounded by photo-multiplier tubes. Electron anti-neutrinos are detected by means of the inverse beta decay $\bar{\nu}_e + p \rightarrow e^+ + n$ by looking for the e^+ in delayed coincidence with the 2.2MeV γ -ray from the

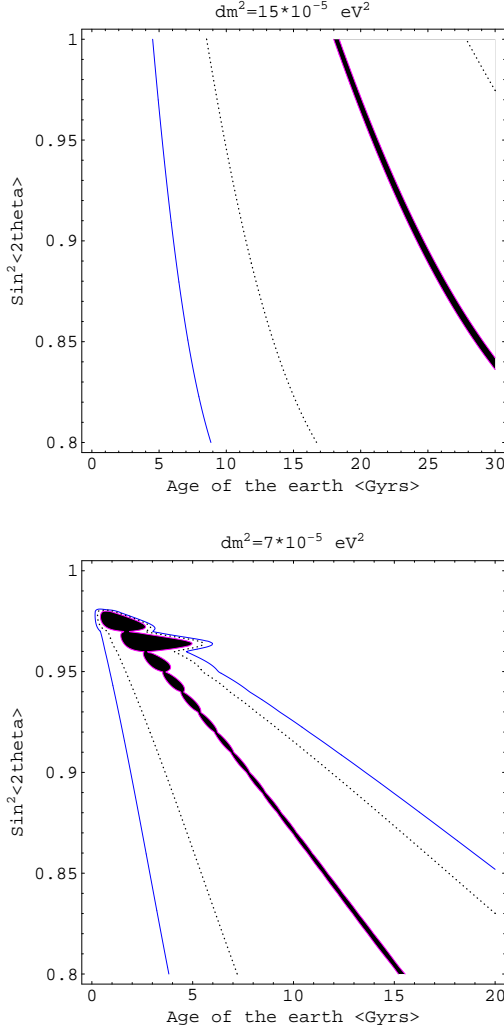


FIG. 1: Age of the earth at 68.3C.L.% (dashed curves) and 90%C.L. (solid curves). Shaded region is the $\chi^2 \simeq 0$ allowed parameter space.

neutron capture by protons ($n + p \rightarrow d + \gamma$). The e^+ annihilate in the detector producing a total visible energy E which is related to the initial $\bar{\nu}_e$ energy, E_ν , as $E = E_\nu - (m_n - m_p + m_e) + 2m_e = E_\nu - 0.78 \text{ MeV}$. Only those radioactive product $\bar{\nu}_e$'s with energies above the inverse beta decay reaction threshold of $m_n - m_p + m_e = 1.8 \text{ MeV}$ can be detected. The main source of $\bar{\nu}_e$'s and radiogenic heat in the earth are decays of ^{238}U , ^{232}Th and ^{40}K . The $\bar{\nu}_e$ from ^{40}K decay have $E_{\nu\text{max}} = 1.31 \text{ MeV}$ and will not register in the KamLAND detector. In the decay chain of ^{238}U , only $\bar{\nu}_e$'s from the β decays of ^{234}Pa and ^{214}Bi are above the threshold for detection in KamLAND. In the ^{232}Th decay chain, $\bar{\nu}_e$'s from the beta decays of ^{228}Ac ^{212}Bi contribute to the KamLAND signal. Thorium decay $\bar{\nu}_e$'s will contribute only to the (positron signal) energy bins below 1.5 MeV whereas Uranium $\bar{\nu}_e$'s will contribute to all energy bins below $E = 2.5 \text{ MeV}$. This fact enables us to separate the thorium neutrino

signal from that of uranium. The energy spectrum of $\bar{\nu}_e$'s from each of these beta decays can be expressed analytically as follows,

$$\eta_X(E) = \sum A(Q, Z) \times F(Z, E_\nu) \times E_\nu^2 (Q + m_e - E_\nu) [(Q + m_e - E_\nu)^2 - m_e^2]^{1/2} \quad (1)$$

where $F(Z, E_\nu)$ is the Fermi function that accounts for the distortion of the spectrum due to Coulomb attraction of the outgoing e^- with the nucleus, the sum is over each of the beta decays in the X ($= Th, U$) decay chain with Q value above the 1.8 MeV threshold, $A(Q, Z)$ are constants obtained by the normalizing the spectrum for each term in the sum to unity. The remaining terms are kinematical factors for the two body decay (assuming the recoil energy of the nucleus is negligible). Other nuclear physics effects can be parameterized by adjusting the overall normalization to match the tabulated experimental values [13] (we fit the normalization of U and Th spectrum by requiring that $I = \int dE \sigma(E) \eta(E) = 0.51$ $(2.52) \times 10^{-44} \text{ cm}^2$ for Thorium (Uranium) where σ is the inverse beta decay cross section shown in (9) below.

The neutrino flux from the earth at a location \vec{R}_d of the detector can be expressed as the integral

$$\Phi_\nu(\vec{R}_d) = \frac{1}{4\pi} \int d^3r \frac{1}{|\vec{r} - \vec{R}_d|^2} \frac{n_X(\vec{r})}{\tau_X} P_{ee}(|\vec{r} - \vec{R}_d|) \quad (2)$$

where $n_X(\vec{r})$ is the number density of the radioactive atoms X ($= U, Th$) and τ_X is the lifetime of X and $P_{ee}(|\vec{r} - \vec{R}_d|)$ is the $\bar{\nu}_e$ survival probability. Assuming that $n_X(\vec{r})$ is approximately constant within a spherical shell, the expression for the flux from a shell of constant density of radioactive atoms can then be written as

$$\Phi_\nu = \frac{G_i}{4\pi R_e^2} \frac{M_i [X]_i}{\tau_X} \quad (3)$$

where $[X]_i$ is the number of X atoms per unit mass in the shell i , M_i is the mass of the i 'th shell and R_e is the radius of the earth. The geometrical factor G_i depends upon the thickness of the shell at the site of the detector and is given by

$$G_i = \frac{3}{2} \frac{1}{(x_2^3 - x_1^3)} \int_{x_1}^{x_2} dx \int_{-1}^1 d\mu \frac{x^2}{1 + x^2 - 2\mu x} P_{ee} \quad (4)$$

where $x_1 = r_1/R_e$, $x_2 = r_2/R_e$ are the inner and outer radii of the shell in units of R_e , μ is the cosine of the angle between the position of the detector, \vec{R}_d , and a point \vec{r} inside the shell (the origin of the coordinates is chosen at the center of the earth). The survival probability of $\bar{\nu}_e$ is a function of the distance between the detector and the point \vec{x} in the shell and is given explicitly by

$$P_{ee} = 1 - \sin^2 2\theta \sin^2 \left[\frac{\Delta m^2 R_e}{4E_\nu} (1 + x^2 - 2\mu x)^{1/2} \right] \quad (5)$$

Inserting P_{ee} in the expression for the geometrical factor and carrying out the integration over the shell thickness x and the angular variable μ , we can express the energy dependence of G_i as

$$G_i(E) = G_i(0) \left(1 - \frac{1}{2} \sin^2 2\theta \times f_i(E)\right) \quad (6)$$

where $G_i(0)$ depends on the shell thickness and $f_i(E)$ is slowly varying function of E (when $\Delta m^2 \simeq 10^{-4} - 10^{-5} \text{eV}^2$). For the continental crust, with thickness 30km , $G_{cc}(0) = 3.54$ and $f_{cc}(E)$ is a monotonically decreasing function of the positron signal energy, E , with $f_{cc}(0.9) = 1.00$ and $f_{cc}(2.5) = 0.98$. For the oceanic crust with thickness of about 6km , $G_{oc} = 4.34$ and $f_{oc}(E)$ decreases monotonically from $f_{oc}(0.9) = 0.88$ to $f_{oc}(2.5) = 0.82$. For neutrinos coming from the mantle, there is an energy independent suppression, and we have $G_m(0) = 1.5$ with $f_m(E) = 1$.

The total contribution to the neutrino flux from the crust and mantle can be written as

$$\Phi_\nu = \left(\frac{\eta_U(E)}{\tau_U} + \left[\frac{Th}{U} \right] \frac{\eta_{Th}(E)}{\tau_{Th}} \right) \left[\sum_i M_i [U]_i g_i G_i(E) \right]$$

where the index $i = cc, oc, m$ denotes the continental crust, oceanic crust and mantle respectively. In the absence of significant chemical segregation of U and Th the ratio $([Th]_i/[U]_i)$ can be taken to be the same in the crust and the mantle. g_i is the location parameter which represents the fraction of the continental crust *vis-a-vis* the oceanic crust surrounding the detector. For a detector in Japan which has the oceanic crust on one side and the Asian continental crust on the other side we may take $g_{cc} \sim g_{oc} \sim 0.5$.

The number of detection events N_i in an energy bin centered at i is,

$$N_i = (n_p t d_{eff}) \int_{i-\epsilon/2}^{i+\epsilon/2} dE \sigma(E) \eta_X(E) \Phi_\nu \quad (8)$$

where n_p number of free target protons in the fiducial volume (3.46×10^{31} for this experiment), t is the exposure time (145.1days) and d_{eff} is the detector efficiency (78.3%) and ϵ is the width of the energy bins (0.425MeV). The low energy cutoff in KamLAND is 0.9MeV .

The cross section for the $\bar{\nu}_e + p \rightarrow e^+ + n$ reaction is given by [14]

$$\sigma = 0.0952 \left(\frac{E_e p_e}{\text{MeV}^2} \right) \times 10^{-42} \text{cm}^2 \quad (9)$$

where $E_e = E_\nu - (m_n - m_p)$ is the positron energy and p_e is the corresponding momentum. Thorium neutrinos have a $E < 1.5 \text{MeV}$, whereas Uranium neutrinos contribute in the entire range of $(E_{min} - 2.5) \text{MeV}$ (where $E_{min} = 0.9$ is the threshold of the lowest energy bin).

The ratio of the neutrino events in the energy bins between $(E_{min} - 1.5) \text{MeV}$, N_I , and the events in energy bins $(1.5 - 2.5) \text{MeV}$, N_{II} , depends only on the Thorium to Uranium ratio $[Th]/[U]$, and the spectral shape of U and Th neutrinos folded with the cross section. The geology factor in the square brackets in (7) cancels out as it is independent of energy (to $\pm 1\%$). Specifically the ratio of the geo-neutrino events in the two energy ranges can be written in a simple form

$$\frac{N_I}{N_{II}} = \alpha + \left[\frac{Th}{U} \right] \times \beta \quad (10)$$

where

$$\alpha = \frac{\int_{E_{min}}^{1.5} dE \sigma(E) \eta_U(E)}{\int_{1.5}^{2.5} dE \sigma(E) \eta_U(E)} = 0.89 \quad (11)$$

and

$$\beta = \frac{\tau_U}{\tau_{Th}} \frac{\int_{E_{min}}^{1.5} dE \sigma(E) \eta_{Th}(E)}{\int_{1.5}^{2.5} dE \sigma(E) \eta_U(E)} = 0.12 \quad (12)$$

One can determine the ratio N_I/N_{II} and from that determine the global average abundance ratio of Th by (7)U using 10. From the initial r-process abundance [10] $[Th/U]_0 = 1.169 \pm 0.08(1\sigma)$ and the decay lifetimes of U and Th ($\tau_U = 6.45 \text{Gyrs}$, $\tau_{Th} = 20.03 \text{Gyrs}$) we can relate the time elapsed (in Giga-years) between the supernova explosion where the earths U, Th were formed and the present,

$$[Th/U] = [Th/U]_0 \exp[t_{age} \left(\frac{1}{6.45} - \frac{1}{20.03} \right)] \quad (13)$$

We can directly relate the age of the earth to the experimentally measured quantity N_I/N_{II} as

$$t_{age} = 9.45 \ln \left[\frac{1}{\beta [Th/U]_0} \left(\frac{N_I}{N_{II}} - \alpha \right) \right] \text{Gyrs} \quad (14)$$

We calculate the reactor background using the procedure given in [15]. We sum the neutrino flux from 16 reactors using their power production and distances as input and assuming an average fuel composition in the ratio $^{235}\text{U} : ^{238}\text{U} : ^{239}\text{Pu} : ^{241}\text{Pu} :: 0.568 : 0.078 : 0.297 : 0.057$. The reactor neutrino flux is shown in Fig 2. We see that there although there is a significant difference between the reactor flux for the LMA-I and LMA-II solutions [11] in the geo-neutrinos energy regime.

The Kamland experiment reports the events in $(0.9 - 1.75) \text{MeV}$ and $(1.75 - 2.6) \text{MeV}$ energy. Using the theoretical spectrum of the Th and U geo-neutrinos we have distributed the 67% of the events in the $(0.9 - 1.75) \text{MeV}$ bin to $(0.9 - 1.5) \text{MeV}$ and 33% of this bin have been assigned to the $(1.5 - 2.5) \text{MeV}$ events. In the $(0.9 - 1.5) \text{MeV}$ energy range LMA-II reactor neutrinos are more suppressed than LMA-I, while in the $(1.5 - 2.5) \text{MeV}$ energy range the LMA-I reactor neutrinos are more suppressed than LMA-II. After this reactor signal is subtracted from the KamLAND observed

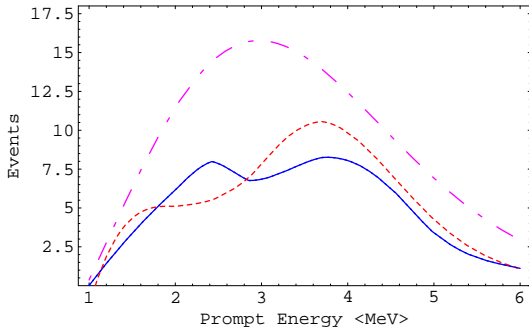


FIG. 2: Reactor neutrino flux. Dash-dot no oscillation, dotted- LMA-I, continuous LMA-II.

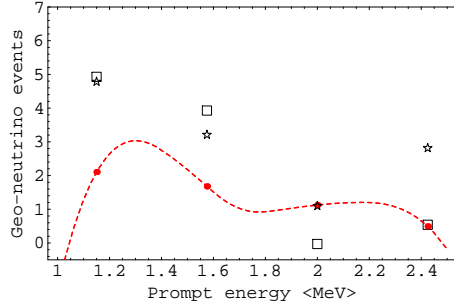


FIG. 3: Simulated geo-neutrino events shown connected with dotted lines. Stars (LMA-I) and squares (LMA-II) denote observed events at KamLAND minus the reactor background.

events, the ratio of geo events in the two energy windows, N_I/N_{II} will go up as we go from LMA-I to LMA-II.

In Fig 3. we plot the simulated geo-neutrino events shown by points connected by dotted line - where we have used the input values of $[Th/U] = 3.8$, $\sin^2 2\theta = 0.88$, $M_{cc}(U) = 4.2 \times 10^{17} kg$, $M_{oc}(U) = 4.8 \times 10^{15} kg$ and

$M_m(U) = 1.23 \times 10^{17} kg$. The geo-neutrino events have no dependence on Δm^2 . In the same figure we have show the experimental points (Kamland events minus the reactor background) where stars represent LMA-I and squares represent LMA-II. Both the LMA-I and LMA-II data points agree with the geo-signal within the 1σ error bars of the KamLAND data points. The N_I/N_{II} ratio which can be read off from the graph is considerably large for the LMA-II points compared to the LMA-I points which leads to a large value of t_{age} for LMA-II compared to LMA-I. The error in determination of t_{age} from KamLAND is estimated as follows. The systematic error in each of N_I and N_{II} from Table II of [1] is 6.4%. The combined systematic and statistical error in N_I is 25% and in N_{II} it is 26%. The total systematic and statistical error in determination of N_I/N_{II} is 36%. The theoretical uncertainty in the initial r-process prediction of $[Th/U]$ is 5%. The assumption that the geometrical factor $G_i(E)$ is energy independent introduces an error of 1%. Added in quadrature the total error in t_{age} is turns out to be 36.5%. With this error we plot the 90% and 68.3% allowed region for t_{age} as a function of mixing angle in Fig 1. We see that the LMA-II solution does not overlap with the solar system age of $4.5 Gyr$ s at 90% C.L.. We emphasize that the LMA-II data points fit the geo events in KamLAND, its the extra constraint of requiring $N_I/N_{II} \sim 1.13$ (which amounts to $t_{age} = 4.5 Gyr$ s) which the LMA-II solution does not fulfill. We must add the cautionary caveat that although there is a large magnification in the ratio N_I/N_{II} in going from LMA-I to LMA-II, this ratio is meaningful when N_I and N_{II} are non-zero. The present KamLAND observations [1] of geo-neutrino events are consistent with zero at 2σ , so the conclusions derived in this paper should be treated as 1σ results.

Acknowledgments I thank Anjan Joshipura for his help and for valuable discussions at every stage of this work.

-
- [1] K.Eguchi et al., KamLAND Collaboration, hep-ex/0212021.
[2] G.Eder, Nucl. Phys. **78**,657 (1966); G.Marx, Czech.J.Phys.B,**19**,1471(1969); C.Avilez, et al. Phys. Rev.D. **23**,1116 (1981).
[3] L.M.Krauss et al.,Nature,**310**,191(1984).
[4] M.Kobayashi and Y.Fukao, Geophys. Res. Lett. **18** 633 (1991).
[5] C.G.Rothschild, M.C.Chen and F.P. Calaprice, Geophys. Res. Lett. **25** 1083(1998).
[6] R.S.Raghavan et al., Phys. Rev. Lett. **80**, 635 (1998).
[7] G.Fiorentini, F.Mantovani and B. Ricci, nucl-ex/0212008.
[8] G.Fiorentini et al., hep-ph/0301042.
[9] D.Arnett, *Supernovae and nucleosynthesis*, Princeton Univ. Press, Princeton, NJ, 1996.
[10] K.Otsuki, G.J.Mathews, K.Toshitaka, astro-ph/0207596.
[11] V. Barger et al. hep-ph/02122126; G.L.Fogli et al hep-ph/0212127; A.Bandopadhyay et al. hep-ph/0212146 ; J.N.Bahcall et al. hep-ph/0212147; H.Nunokawa et al. hep-ph/0212202; P.C.Hollanda et al. hep-ph/0212270 ; M. Maltoni, T. Schwetz, J.W.F. Valle, hep-ph/0212129; M.Maltoni,T. Schwetz,M.A. Tortola,J.W.F.Valle. Phys.Rev.D67:013011,2003.
[12] E.Andres and N.Grevesse, Geochim. Cosmochim. Acta **53**,191 (1989);S.Hart and A.Zindler, Chem. Geol. **57**,247 (1986).
[13] H. Behrens and J. Janecke, *Numerical tables for Beta-Decay and Electron Capture*, Springer Verlag, Berlin,1969.
[14] C.Bemporad, G.Gratta and P.Vogel, Rev. Mod. Phys. **74**, 297 (2002); P.Vogel and J.F.Beacom, Phys. rev. **D60**, 053003(1999).
[15] H.Murayama and A.Pierce, Phys. Rev **D 65**,013012 (2002).